Vibrational Dephasing of Carbonmonoxy Myoglobin

Ryan B. Williams and Roger F. Loring*

Department of Chemistry and Chemical Biology, Baker Laboratory, Cornell University, Ithaca, New York 14853

M. D. Fayer

Department of Chemistry, Stanford University, Stanford, California 94305

Received: March 1, 2001; In Final Form: March 30, 2001

The autocorrelation function of vibrational frequency fluctuations of the CO ligand in carbonmonoxy myoglobin, $C_{\delta\delta}(t)$, is computed from molecular dynamics simulations. Electrostatic interactions are assumed to dominate the modulation of the CO vibrational frequency. The simulated $C_{\delta\delta}(t)$ is consistent with linear and nonlinear infrared spectroscopic measurements. The short-time decay of $C_{\delta\delta}$ is dominated by dynamics of the distal histidine, and of a water molecule that can occupy the heme pocket. Correlated protein and solvent dynamics induce spectral diffusion of the CO frequency on longer time scales.

Introduction

Protein dynamics on a wide range of time scales promote biological function. Motions on the shortest time scales of femtoseconds to nanoseconds are of intrinsic importance and can also act as the fluctuations that drive processes on longer time scales. A novel class of nonlinear vibrational spectroscopic techniques,[1−4] which are analogs of multidimensional magnetic resonance spectroscopy, can provide a direct measure of such protein structural fluctuations. These measurements include the two-pulse and three-pulse infrared vibrational echoes, which have been applied to ligands bound to heme proteins by Fayer and co-workers[5−10] and by Hochstrasser and co-workers.[11−14] The two-pulse vibrational echo, like its optical and magnetic resonance predecessors, has the capability to extract a homogeneous dephasing time, T_2, for a vibrational transition that is inhomogeneously broadened. Two-pulse echoes can also probe spectral diffusion processes on longer time scales,[9,10] which are directly interrogated by the three-pulse echo.[11−15] Vibrational echo measurements have been usefully described in terms of phenomenological stochastic models,[9,10] but a molecular interpretation requires an atomistic calculation of the nonlinear vibrational response[16−18] determined in these experiments.

Myoglobin is a standard for the study, in the laboratory[19−21] and on the computer,[22−26] of relationships among protein structure, function, and dynamics. Fayer and co-workers[5−10] have performed vibrational echo studies on the dephasing of the CO vibration in carbonmonoxy myoglobin, MbCO, and have established the dependence of this dephasing rate on temperature, solvent viscosity, and mutations. The dependence of T_2 on solvent viscosity[9,10] demonstrates the influence of solvent dynamics on protein motions and shows that the vibrational dynamics of the CO ligand are influenced by motions of the entire protein.

In this work, we use molecular dynamics simulations to compute the ligand dephasing dynamics of MbCO in water at 300 K within a consistently classical mechanical approach. We employ a strategy that we denote the fluctuating frequency approximation,[17] in which an oscillator with cubic anharmonicity is represented as a harmonic oscillator with a time-dependent fluctuating frequency. This is a well-established approximation for the calculation of the linear response[27−29] of a classical or quantum mechanical oscillator and has been recently generalized to treat the classical mechanical nonlinear response.[17] Within this approximation, the fluctuation in the oscillator frequency is expressed as $\delta\omega(t) \equiv f\,\delta F(t)/(2m^2\omega^3)$, with f the cubic anharmonicity, $\delta F(t)$ the fluctuation in the component of the classical force on the oscillator coordinate, m, the reduced mass, and ω the harmonic frequency. Within the further approximation that $\delta\omega(t)$ is a Gaussian stochastic variable, both linear and nonlinear response functions[17,30] may be expressed in terms of the autocorrelation function of the vibrational frequency fluctuation, $C_{\delta\delta}(t) \equiv \langle\delta\omega(t)\delta\omega(0)\rangle$, with the angle brackets representing a classical ensemble average.

We assume that the dominant contribution to $\delta\omega(t)$ in MbCO is from electrostatic interactions between the ligand and its surroundings.[19,24,31] These are represented by the interaction of the electric dipole of the CO, assumed to be linear in bond coordinate, with $\mathbf{E}(t)$, the total electric field at the midpoint of the CO bond from the surrounding protein and solvent. $\delta\omega$ takes the form

$$\delta\omega(t) = A[\mathbf{E}(t)\cdot\mathbf{u}(t) - \langle\mathbf{E}\cdot\mathbf{u}\rangle] \tag{1}$$

$$A \equiv \frac{f(\mathrm{d}\mu/\mathrm{d}q)_0}{2m^2\omega^3} \tag{2}$$

The unit vector along the CO dipole is denoted $\mathbf{u}(t)$, with time dependence arising from orientational dynamics, and the coordinate derivative of the dipole moment at the potential minimum is $(\mathrm{d}\mu/\mathrm{d}q)_0$. Direct calculation of $\delta\omega(t)$ from a simulation would require a bond potential for CO in MbCO with accurate values of bond anharmonicity f and dipole derivative $(\mathrm{d}\mu/\mathrm{d}q)_0$. Instead, we exploit the fact that A in eq 2 may be measured with vibrational Stark spectroscopy. To first-order quantum mechanical perturbation theory in both bond anharmonicity and field-matter interaction, $A = \Delta\mu/\hbar$, with $\Delta\mu$ the magnitude of the electric dipole difference between first excited and ground vibrational states.[32] While $\Delta\mu$ is a quantum

10.1021/jp010798o CCC: $20.00
Published on Web 04/24/2001

mechanical quantity, A is independent of $\hbar$ and hence is an appropriate input to our classical calculation. Park et al.[33] have performed vibrational Stark effect measurements on CO as a ligand in a series of Mb mutants and other heme species and have measured $\Delta\mu$ of approximately 0.14 D, oriented along the permanent dipole moment of CO. The small variation in this result across a range of Mb mutants and other heme species motivates the conjecture[33] that the local field correction of vibrational Stark spectroscopy is not large, and we will neglect this correction here. We determine $C_{\delta\delta}(t)$ from eq 1 by calculating the time-dependent electric field at the CO ligand from molecular dynamics simulations and by employing the value of A determined experimentally.[33]

Results and Conclusions

A solvated molecule of sperm whale carbonmonoxy myoglobin was simulated using the program MOIL.[34] The fully equilibrated structure was obtained from a previous study of CO photodissociation in MbCO by Meller and Elber.[24] The 40 Å × 54 Å × 56 Å simulation box treated with periodic boundary conditions contains one myoglobin molecule, one CO bound[35] to the heme iron, 2627 H_2O, one SO_4^{2-} present in the crystal structure, and two Na^+ to balance the system charge. From the initial equilibrated structure,[24] a 300 ps equilibration was performed in which a water molecule initially in the heme pocket leaves the pocket after 180 ps. The departure of the water molecule from the heme pocket is defined to occur when the distance between the oxygen atom of the water molecule and the midpoint of the CO bond exceeds 10 Å. Two additional equilibration runs were launched from configurations with the water in the pocket and a configuration with the water absent. Each secondary equilibration lasted 200 ps for a total of 700 ps of equilibration. Equilibrium structures used in subsequent production runs were separated by at least 5 ps and designated IN and OUT based on the location of the heme pocket water. Coordinates were saved every 20 fs and a time step of 1.0 fs was used for all simulations. The production runs totalled 3.35 ns from 30 different initial IN configurations and 3.30 ns from 36 different initial OUT configurations. Only twice in the entire simulation time including equilibration did the water initially inside the pocket depart and only once did the water molecule return to the pocket from outside the 10 Å radius. The statistical weights of IN and OUT configurations cannot be determined from less than 7 ns of simulation. These two cases will be treated separately. As discussed below, the presence of a water molecule in the heme pocket has a substantial effect on the short time decay of $C_{\delta\delta}(t)$, providing a rationale to treat the IN and OUT cases as spectroscopically distinct structures.

Because vibrational echo experiments[5−10] probe only the A_1 state of the CO vibrational band, trajectories in which the distal histidine assumes a conformation associated with the A_0 state[25] were discontinued once this event occurred. Configurations were deemed to correspond to the A_0 band if the distance of the H atom bonded to N_δ on the distal histidine exceeded a distance of 6.5 Å from the midpoint of the CO bond.[25] This event occurred infrequently as the protonated nitrogen tends to align itself toward the CO. This procedure resulted in 2.95 ns of OUT and 2.84 ns of IN trajectories that were used to calculate $C_{\delta\delta}(t)$.

For each structure saved during the trajectories, an electric field vector is calculated at the midpoint of the CO bond from Coulomb's law and atomic partial charges.[34] The orientation of the CO dipole $\mathbf{u}(t)$ is also computed for a given structure and combined with the electric field in eq 1 to yield the CO frequency fluctuation as a function of time. $C_{\delta\delta}$ is then computed for both IN and OUT cases as shown in Figure 1. The IN case is shown by the solid line, and the OUT case is shown by dots. $C_{\delta\delta}$ for the IN and OUT cases differ appreciably for $t < 100$ fs. For $t > 7$ ps, the correlation functions are similar, with a long time decay that does not reach zero on the time scale shown. Both functions were fit to a biexponential decay of the form[12]

$$\langle \delta\omega(t)\, \delta\omega(0)\rangle \approx \sum_{i=1}^{2} \Delta_i^{\,2} \exp\left[\frac{-t}{\tau_i}\right] + \Delta_0^{\,2} \qquad (3)$$

with the parameters given in the first two rows of Table 1. Frequency fluctuations in CO are characterized by a fast process of amplitude Δ_1 and time scale τ_1 that obeys the motional narrowing criterion $\Delta_1\tau_1 < 1$, a process of intermediate time scale of amplitude Δ_2 and time scale τ_2 that is in the regime of spectral diffusion $\Delta_2\tau_2 > 1$, and a slow process of magnitude Δ_0 that is static on the simulated time scales. As shown in Table 1, τ_2, Δ_2, and Δ_0 are similar for the IN and OUT cases. The magnitude of short time scale fluctuations, Δ_1, is larger and the associated decay time, τ_1, is shorter when the water molecule is inside the heme pocket.

The simulated $C_{\delta\delta}(t)$ for the IN and OUT cases of MbCO are compared in Table 1 to $C_{\delta\delta}(t)$ for carbonmonoxy hemoglobin (HbCO) in water at 300 K, deduced from three-pulse vibrational echo experiments by Lim et al.[12] The frequency fluctuations computed for MbCO are larger than those reported for HbCO, and both τ_1 and τ_2 are shorter for MbCO than for HbCO. This comparison is consistent with the broader vibrational absorption line shape[8,10] in MbCO (∼17 cm^{-1}) relative to that[12] in HbCO (∼8 cm^{-1}), and with vibrational echo measurements[8] that

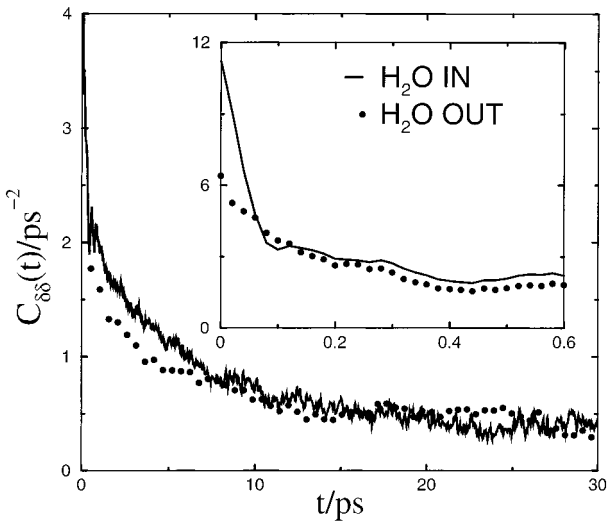

Figure 1. Autocorrelation function of CO frequency fluctuations in MbCO is shown for two cases. The solid lines show $C_{\delta\delta}(t)$ with a water molecule occupying the heme pocket (IN), and dots represent $C_{\delta\delta}(t)$ in the absence of this water molecule (OUT). The inset displays the short time decay for both cases.

TABLE 1: Parameters in Eq 1 for $C_{\delta\delta}(t)$ in Figure 1[a]

case (molecule)	Δ_1, ps^{-1}	τ_1, ps	Δ_2, ps^{-1}	τ_2, ps	Δ_0, ps^{-1}
OUT (MbCO)	2.07	0.14	1.14	4.95	0.67
IN (MbCO)	3.08	0.05	1.38	5.12	0.64
(HbCO)	0.71	0.5	0.41	12	0.35

[a] The third row shows a fit[12] to data from 3-pulse echo experiments[12] on HbCO in water at 300 K.

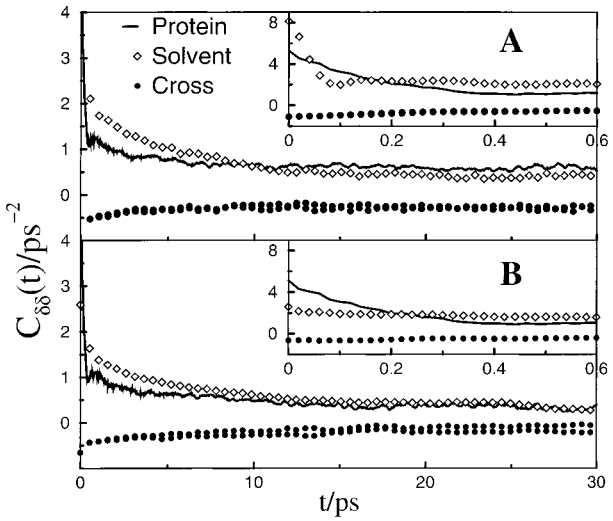

Figure 2. $C_{\delta\delta}(t)$ computed from the electric field of the protein is shown by solid lines. Diamonds indicate $C_{\delta\delta}(t)$ computed from the solvent electric field, and cross-correlation functions of the protein and solvent contributions are plotted with dotted lines. Panel A corresponds to the IN case, while panel B indicates the OUT case, and the insets show short time behavior for all functions.

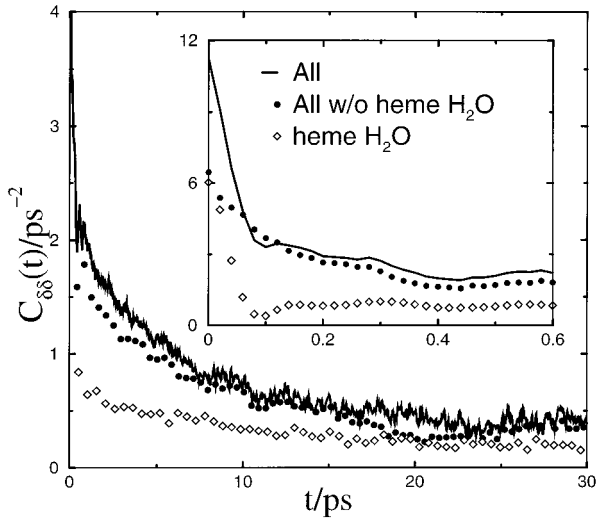

Figure 3. $C_{\delta\delta}(t)$ is computed from the electric field at CO from the entire system (solid line), from the heme pocket water (diamonds), and from the system excluding the contribution of this water molecule (dotted line). Cross-correlations between contributions from the heme pocket water and the rest of the system are negligible and are not shown. The inset shows short time behavior for all functions.

determined dephasing rates in HbCO to be smaller than in MbCO over a wide range of temperature. Absorption line widths[27−29] were calculated for MbCO using $C_{\delta\delta}$ in Figure 1 and the experimental value[5−10] of $T_1 \approx 20$ ps to yield 22.9 cm^{-1} for the IN case and 19.7 cm^{-1} for the OUT case. These line widths show reasonable agreement with the experimental value of $\sim$17 cm^{-1}. Since $\Delta_1\tau_1 < 1$ for both IN and OUT cases, a homogeneous dephasing rate, $1/T_2 = \Delta_1^2\tau_1$, can be calculated to yield $1/T_2 = 0.47$ ps^{-1} for the IN case and $1/T_2 = 0.60$ ps^{-1} for the OUT case. Both results are consistent with the experimental value of $1/T_2 = 0.67$ ps^{-1} as measured by two-pulse vibrational echo experiments.[9,10]

To determine the molecular origin of each dephasing process in Table 1, we partition the total electric field vector at the midpoint of the CO bond into contributions from partial charges on different parts of the protein and solvent. Substitution of this partitioned electric field into eq 1 yields a partitioning of the fluctuating frequency of CO into contributions from different sources. Autocorrelations and cross-correlations of these contributions to $\delta\omega(t)$ are then determined. We begin by dividing the total electric field at CO into a contribution from the protein that produces a frequency fluctuation $\delta\omega_p(t)$, and a contribution from all water molecules that produces a frequency fluctuation $\delta\omega_h(t)$. The resulting correlation functions are shown in Figure 2 for both IN (panel A) and OUT (panel B) cases. $\langle\delta\omega_p(t)\ \delta\omega_p(0)\rangle$ is shown by solid lines, and $\langle\delta\omega_h(t)\ \delta\omega_h(0)\rangle$ is given by diamonds. $\delta\omega_p$ includes contributions from the heme ring and Fe. While the heme ring and Fe cause a sizable static electric field at CO, they make a negligible contribution to the field fluctuations that cause dephasing. The cross-correlation functions $\langle\delta\omega_p(t)\ \delta\omega_h(0)\rangle$ and $\langle\delta\omega_h(t)\ \delta\omega_p(0)\rangle$ are shown by dotted lines and are sufficiently similar that we do not distinguish between them. $\langle\delta\omega_p(t)\ \delta\omega_p(0)\rangle$ is similar in the IN and OUT cases, especially on the short time scales depicted in the insets. The protein is responsible for the initial decay in the OUT case, while the water produces an additional rapid decay in the IN case. Both panels show that water and protein contribute to the intermediate time scale spectral diffusion and the long time scale inhomogeneous broadening. After 10 ps, $\langle\delta\omega_h(t)\ \delta\omega_h(0)\rangle$ in the OUT case decays on a time scale similar to that of $\langle\delta\omega_p(t)\ \delta\omega_p(0)\rangle$, suggesting that the dynamics of the water is influenced by interactions with the protein. The slow decay from negative values of $\langle\delta\omega_p(t)\ \delta\omega_h(0)\rangle$ demonstrates the influence on the CO of correlated protein and water dynamics.

Figure 3 shows the results of a similar partitioning of the total electric field at CO for the IN case into the contribution from the single water molecule in the heme pocket and from the rest of the system, composed of the remaining water molecules and the protein. The solid line is the total correlation function repeated from Figure 1, the diamonds are computed from the electric field due to the single water in the heme pocket, and the dotted line shows $C_{\delta\delta}$ from the rest of the system. Cross-correlations between the contributions to $\delta\omega$ from the heme pocket water and the rest of the system are negligible on all time scales and are not shown. From the inset it is evident that the single water molecule in the heme pocket produces the most rapid portion of the total IN correlation function. This is also evident from Figure 1, which shows that the initial decay in the IN case disappears when the water has moved out of the pocket. The total correlation function at longer time scales shows a small contribution from the heme pocket water, suggesting different water configurations in the heme pocket lead to a portion of the inhomogeneous line width. When a water molecule occupies the heme pocket, it exerts rapid electric field fluctuations on the ligand frequency, causing increased motional narrowing. In addition, different orientations and positions of the water in the heme pocket contribute to long time inhomogeneity.

In Figure 4, the electric field at CO from just the protein, excluding the contribution from all water molecules, was further partitioned into that arising from the distal histidine and that from the rest of the protein. Panel A (IN) and panel B (OUT) display $C_{\delta\delta}$ from the entire protein (also shown in Figure 2) with solid lines, $C_{\delta\delta}$ from just the distal histidine with diamonds, and $C_{\delta\delta}$ from the rest of the protein, excluding the distal histidine, with dotted lines. The cross-correlations between the histidine contribution and that from the rest of the protein are negligible and are not shown. Both panels show that the electric field at CO from the distal histidine accounts for almost all of the short time behavior of the total protein contribution to $C_{\delta\delta}$.

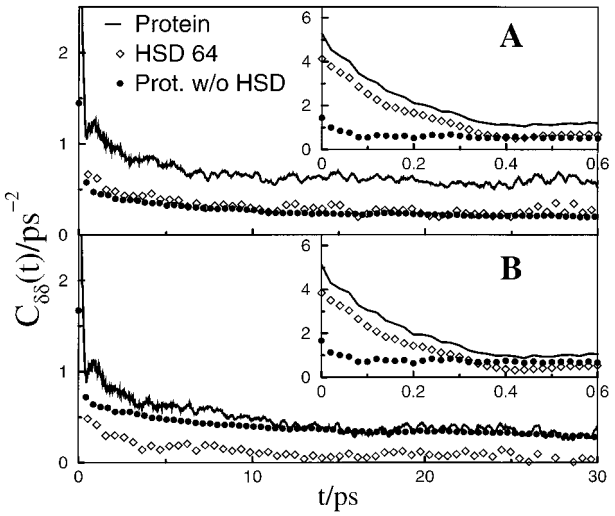

Figure 4. $C_{\delta\delta}(t)$ is computed from the electric field of the protein (solid line), the electric field of the distal histidine (diamonds), and the electric field of the protein excluding the contribution of the distal histidine (dotted line). Cross-correlations between contributions from the distal histidine and from the rest of the protein are negligible and are not shown. Panel A corresponds to the IN case, while panel B indicates the OUT case, and the insets show short time behavior for all functions.

There is also a longer time scale decay of the histidine contribution in both cases that is on the order of τ_2 in Table 1. Figure 4 shows that the distal histidine contributes to dephasing in both the motional narrowing and spectral diffusion regimes. This finding is qualitatively consistent with vibrational echo measurements of Rector et al.[5] on the Mb mutant H64V, which showed that replacing the distal histidine with a valine decreased the dephasing rate. The major difference between the two panels in Figure 4 concerns the contribution of the protein to inhomogeneous line broadening. In panel B for the OUT case, the static portion of the total protein contribution to $C_{\delta\delta}$ is almost completely due to contributions from the protein excluding the histidine, while panel A shows that both the histidine and the rest of the protein contribute to this slow process for the IN case. With a water in the heme pocket, the distal histidine and the water assume long-lived configurations that contribute to the inhomogeneous line width.

We have shown that molecular dynamics simulations of MbCO yield a prediction for $C_{\delta\delta}(t)$ that agrees well with linear and nonlinear infrared measurements on all relevant time scales. A water molecule occupying the heme pocket with the bound ligand is found to significantly alter the fastest dynamics of $C_{\delta\delta}(t)$. Dynamics of the distal histidine also affect the short time frequency fluctuations of CO, whether or not a water is present in the heme pocket. Protein and solvent contributions to frequency fluctuations of CO show significant correlations. These correlated protein−solvent motions produce intermediate time scale spectral diffusion of ligand frequencies. Echo measurements are in progress on MbCO in water on the 100 fs time scale that will permit direct comparison with the results presented here. Simulations of the full time dependence of the vibrational echo signal[17] will be presented in a future work.

Acknowledgment. R.B.W. acknowledges the U.S. Department of Education for fellowship support. We thank Prof. Ron Elber for helpful discussions regarding MOIL and myoglobin, and Prof. Vijay Pande for assistance in setting up this project. This research was partially conducted using the resources of the Cornell Theory Center, which receives funding from Cornell University, New York State, federal agencies, and corporate partners. M.D.F. acknowledges a grant from the National Institutes of Health (grant no. 1R01-GM61137) for support of this research.

References and Notes

(1) Vanden Bout, D. A.; Berg, M. *Acc. Chem. Res.* **1997**, *30*, 65.

(2) Mukamel, S.; Piryatinski, A.; Chernyak, V. *Acc. Chem. Res.* **1999**, *32*, 145.

(3) Blank, D. A.; Kaufman, L. J.; Fleming, G. R. *J. Chem. Phys.* **2000**, *113*, 771.

(4) Tokmakoff, A. *J. Phys. Chem. A* **2000**, *104*, 4247.

(5) Rector, K. D.; Rella, C. W.; Kwok, A. S.; Hill, J. R.; Sligar, S. G.; Chien, E. Y. P.; Dlott, D. D.; Fayer, M. D. *J. Phys. Chem. B* **1997**, *101*, 1468.

(6) Rector, K. D.; Engholm, J. R.; Hill, J. R.; Myers, D. J.; Hu, R.; Boxer, S. G.; Dlott, D. D.; Fayer, M. D. *J. Phys. Chem. B* **1998**, *102*, 331.

(7) Rector, K. D.; Engholm, J. R.; Rella, C. W.; Hill, J. R.; Dlott, D. D.; Fayer, M. D. *J. Phys. Chem. A* **1999**, *103*, 2381.

(8) Rector, K. D.; Thompson, D. E.; Merchant, K.; Fayer, M. D. *Chem. Phys. Lett.* **2000**, *316*, 122.

(9) Berg, M. A.; Rector, K. D.; Fayer, M. D. *J. Chem. Phys.* **2000**, *113*, 3233.

(10) Rector, K. D.; Berg, M. A.; Fayer, M. D. *J. Phys. Chem. B* **2001**, *105*, 1081.

(11) Hamm, P.; Lim, M.; Hochstrasser, R. M. *Phys. Rev. Lett.* **1998**, *81*, 5326.

(12) Lim, M.; Hamm, P.; Hochstrasser, R. M. *Proc. Natl. Acad. Sci. U.S.A.* **1998**, *95*, 15315.

(13) Hamm, P.; Lim, M.; DeGrado, W. F.; Hochstrasser, R. M. *J. Phys. Chem. A* **1999**, *103*, 10049.

(14) Asplund, M. C.; Lim, M.; Hochstrasser, R. M. *Chem. Phys. Lett.* **2000**, *323*, 269.

(15) Everett, K. F.; Geva, E.; Skinner, J. L. *J. Chem. Phys.* **2001**, *114*, 1326.

(16) Williams, R. B.; Loring, R. F. *J. Chem. Phys.* **2000**, *113*, 1932.

(17) Williams, R. B.; Loring, R. F. *J. Chem. Phys.* **2000**, *113*, 10655.

(18) Williams, R. B.; Loring, R. F. *Chem. Phys.* **2001**, *266*, 167.

(19) Springer, B. A.; Sligar, S. G.; Olsen, J. S.; Phillips, G. N. *Chem. Rev.* **1994**, *94*, 699.

(20) Krzywda, S.; Murshudov, G. N.; Brzozowski, A. M.; Jaskolski, M.; Scott, E. E.; Klizas, S. A.; Gibson, Q. H.; Olson, J. S.; Wilkinson, A. J. *Biochemistry* **1998**, *37*, 15896.

(21) Sagnella, D. E.; Straub, J. E.; Thirumalai, D.; Jackson, T. A.; Lim, M.; Anfinrud, P. A. *Proc. Natl. Acad. Sci. U.S.A.* **1999**, *96*, 14324.

(22) Ma, J.; Huo, S.; Straub, J. E. *J. Am. Chem. Soc.* **1997**, *119*, 2541.

(23) Sagnella, D. E.; Straub, J. E.; Thirumalai, D. *J. Chem. Phys.* **2000**, *113*, 7702.

(24) Meller, J.; Elber, R. *Biophys. J.* **1998**, *74*, 789.

(25) Schultz, B. G.; Evanseck, J. D. *J. Am. Chem. Soc.* **1999**, *121*, 6444.

(26) Schultz, B. G.; Grubmuller, H.; Evanseck, J. D. *J. Am. Chem. Soc.* **2000**, *122*, 8700.

(27) Oxtoby, D. W. *Annu. Rev. Phys. Chem.* **1981**, *32*, 77.

(28) Schweizer, K.; Chandler, D. *J. Chem. Phys.* **1982**, *76*, 2296.

(29) Tuckerman, M.; Berne, B. J. *J. Chem. Phys.* **1993**, *98*, 7301.

(30) Mukamel, S. *Principles of Nonlinear Optical Spectroscopy*; Oxford University Press: New York, 1995.

(31) Augspurger, J. D.; Dykstra, C. E.; Oldfield, E. *J. Am. Chem. Soc.* **1991**, *113*, 2447.

(32) Bishop, D. A. *J. Chem. Phys.* **1993**, *98*, 3179.

(33) Park, E. S.; Andrews, S. S.; Hu R. B.; Boxer, S. G. *J. Phys. Chem. B* **1999**, *103*, 9813.

(34) Elber, R.; Roitberg, A.; Simmerling, C.; Goldstein, R.; Li, H.; Verkhivker, G.; Keasar, C.; Zhang, J.; Ulitsky, A. *Comput. Phys. Commun.* **1994**, *91*, 159.

(35) CO is represented by the two-site model of ref 24.